Forschung im Ingenieurwesen 66 (2000) 17–23 © Springer-Verlag 2000

On impulsive motion of a vertical plate with heat flux and diffusion of chemically reactive species

R. Muthucumaraswamy, P. Ganesan

Abstract Finite-difference solution of the transient natural convection flow of an incompressible viscous fluid past an impulsively started semi-infinite plate with constant heat flux and mass diffusion is presented here, taking into account the homogeneous chemical reaction of first order. The concentration profiles are compared with the exact solution and are found to be in good agreement. The steady-state velocity, temperature and concentration profiles are shown graphically. It is observed that due to the presence of first order chemical reaction, the velocity decreases with increasing values of the chemical reaction parameter. The local as well as average skin-friction, Nusselt number and Sherwood number are shown graphically.

Wärmeübertragung an einer impulslartig, bewegten vertikalen Platte mit Diffusion chemisch reaktiver Substanzen

Zusammenfassung Die instationäre freie Konvektion eines viskosen, inkompressiblen Fluids an einer impulsartig bewegten Platte mit einer konstanten Wärmestromdichte und überlagerter Diffusion wurde innerhalb dieser Arbeit mit der Finite-Differenzen-Methode untersucht. Eine homogene chemische Reaktion erster Ordnung wird berücksichtigt. Die numerisch ermittelten Konzentrationsprofile sind in guter Übereinstimmung mit der exakten analytischen Lösung. Die Geschwindigkeits-, Temperatur- und Konzentrationsprofile werden für den stationären Zustand graphisch dargestellt. Die örtlichen Geschwindigkeiten weisen aufgrund der betrachteten chemischen Reaktion erster Ordnung geringere Werte auf als im Falle ihrer Abwesenheit. Weiterhin werden die Ergebnisse für die lokalen und mittleren Wandschubspannungen, die Nusselt- und Sherwood- Zahlen vorgestellt und diskutiert.

List of symbols

C'	concentration
C	dimensionless concentration
D	mass diffusion coefficient
Gc	mass Grashof number
Gr	thermal Grashof number
g	accelaration due to gravity
K	dimensionless chemical reaction parameter
K_l	chemical reaction parameter
k	thermal conductivity
Nu_X	dimensionless local Nusselt number
$\overline{\mathrm{Nu}}$	dimensionless average Nusselt number
Pr	Prandtl number
q	heat flux per unit area at the plate
Sc	Schmidt number
Sh_X	dimensionless local Sherwood number
$\overline{\mathrm{Sh}}$	dimensionless average Sherwood number
T'	temperature
T	dimensionless temperature
t'	time
t	dimensionless time
u_0	velocity of the plate
U, V	dimensionless velocity components in X, Y-directions respectively
u, v	velocity components in x, y-directions respectively
X	dimensionless spatial coordinate along the plate
x	spatial coordinate along the plate
Y	dimensionless spatial coordinate normal to the plate
y	spatial coordinate normal to the plate

Greek symbols

α	thermal diffusivity
β	volumetric coefficient of thermal expansion
β^*	volumetric coefficient of expansion with concentration
μ	coefficient of viscosity
ν	kinematic viscosity
τ_X	dimensionless local skin-friction
$\overline{\tau}$	dimensionless average skin-friction

Subscripts

w	conditions on the wall
∞	free stream conditions

Received: 21. August 1999

R. Muthucumaraswamy
Department of Mathematics and Computer Applications,
Sri Venkateswara College of Engineering,
Sriperumbudur 602 105, India,
E-mail: scumary@hotmail.com

P. Ganesan (✉)
Department of Mathematics, Anna University,
Chennai 600 025, India,
E-mail: ganesan@annauniv.edu

1 Introduction

Chemical reactions can be codified as either heterogeneous or homogeneous processes. This depends on whether they occur at an interface or as a single phase volume reaction. A few representative fields of interest in which combined

heat and mass transfer plays an important role, are design of chemical processing equipment, formation and dispersion of fog, distribution of temperature and moisture over agricultural fields and groves of fruit trees, damage of crops due to freezing, food processing and cooling towers. Cooling towers are the cheapest way to cool large quantities of water. They are a very common industrial sight, especially in power plants. The tower is packed with inert material, commonly with wooden slats. Hot water sprayed into the top of the tower trickles down through wood, evaporating as it goes. Air enters the bottom of the tower and rises up through the packing. In smaller towers, the air can be pumped with a fan; in larger ones, it is often allowed to rise by natural convection.

Stokes [1] presented an exact solution to the Navier-Stokes equations, which is the flow of a viscous incompressible fluid past an impulsively started infinite horizontal plate in its own plane. It is often called Rayleigh's problem in the literature. Hall [2] considered the flow past an impulsively started semi-infinite horizontal plate by finite-difference method of a mixed explicit-implicit type, which is convergent and stable and hence it is free from any restrictions on the mesh-size. Following Stokes [1] analysis, Soundalgekar [3] was the first to present an exact solution to the flow of a viscous fluid past an impulsively started infinite isothermal vertical plate. Many transport processes exist in nature and in industrial applications in which the simultaneous heat and mass transfer occur as a result of combined buoyancy effects of thermal diffusion and diffusion of chemical species. However, in nature, along with the free-convection currents caused by temperature differences, the flow is also affected by the differences in concentration. It is found useful in chemical processing industries such as food processing and polymer production. Soundalgekar [4] studied the problem of the flow past an impulsively started isothermal infinite vertical plate with mass transfer effects. Muthucumaraswamy and Ganesan [5] have analysed the above problem numerically. In this study, the plate is considered to be semi-infinite and the dimensionless governing equations are solved using implicit-finite difference scheme of Crank-Nicolson type. Soundalgekar et al. [6] have studied the flow past an impulsively started infinite vertical plate with constant heat flux and mass transfer. Das et al. [7] have studied effects of homogeneous first order chemical reaction on the flow past an impulsively started infinite vertical plate with constant heat flux and mass transfer. The dimensionless governing equations are solved by the usual Laplace-transform technique.

The present investigation, involving the simultaneous effects of heat and mass transfer, is concerned with a numerical study of transient natural convection flow past an impulsively started semi-infinite vertical plate which is subjected to uniform heat flux and diffusion of a chemically reactive species. The fluids considered in this study are air and water. The governing equations are solved by an implicit finite-difference scheme of Crank-Nicolson type. In order to check the accuracy of our numerical results, the present study is compared with available exact solution of Das et al. [7] and they are found to be in good agreement.

2
Mathematical analysis

Here the flow of a viscous incompressible fluid past an impulsively started semi-infinite vertical plate with uniform heat flux and mass diffusion is considered. It is assumed that the effect of viscous dissipation is negligible in energy equation and there is a first order chemical reaction between the diffusing species and the fluid. The x-axis is taken along the semi-infinite plate in the vertically upward direction and the y-axis is taken normal to the plate. Initially, it is assumed that the plate and the fluid are of the same temperature and concentration in a stationary condition. At time $t' > 0$, the plate starts moving impulsively in the vertical direction with constant velocity u_0 against the gravitational field. The rate of temperature and the concentration level near the plate is also raised. It is also assumed that there exists homogeneous first order chemical reaction between the fluid and species concentration. Then under usual Boussinesq's approximation the unsteady flow past semi-infinite vertical plate is governed by the following equations

$$\frac{\partial u}{\partial x} + \frac{\partial v}{\partial y} = 0 \tag{1}$$

$$\frac{\partial u}{\partial t'} + u\frac{\partial u}{\partial x} + v\frac{\partial u}{\partial y} = g\beta(T' - T'_\infty) + g\beta^*(C' - C'_\infty) + \nu\frac{\partial^2 u}{\partial y^2} \tag{2}$$

$$\frac{\partial T'}{\partial t'} + u\frac{\partial T'}{\partial x} + v\frac{\partial T'}{\partial y} = \alpha\ \frac{\partial^2 T'}{\partial y^2} \tag{3}$$

$$\frac{\partial C'}{\partial t'} + u\frac{\partial C'}{\partial x} + v\frac{\partial C'}{\partial y} = D\ \frac{\partial^2 C'}{\partial y^2} - \ K_l C' \ . \tag{4}$$

The initial and boundary conditions are

$$\begin{aligned} &t' \le 0: \quad u = 0,\ \ v = 0,\ \ T' = T'_\infty,\ \ C' = C'_\infty \\ &t' > 0: \quad u = u_0,\ \ v = 0, \\ &\qquad\qquad \frac{\partial T'}{\partial y} = -\ \frac{q}{k},\ \ C' = C'_w \quad \text{at } y = 0 \\ &u = 0,\ \ T' = T'_\infty,\ \ C' = C'_\infty \qquad \text{at } x = 0 \\ &u \to 0,\ \ T' \to T'_\infty,\ C' \to C'_\infty \qquad \text{as } y \to \infty \ . \end{aligned} \tag{5}$$

On introducing the following non-dimensional quantities

$$\begin{aligned} &X = \frac{xu_0}{\nu},\ \ Y = \frac{yu_0}{\nu},\ \ U = \frac{u}{u_0},\ \ V = \frac{v}{u_0},\ \ t = \frac{t'u_0^2}{\nu} \\ &T = \frac{T' - T'_\infty}{\left(\frac{q\nu}{ku_0}\right)},\ \ \mathrm{Gr} = \frac{g\beta q\nu^2}{ku_0^4}, \\ &C = \frac{C' - C'_\infty}{C'_w - C'_\infty},\ \ \mathrm{Gc} = \frac{\nu g\beta^*(C'_w - C'_\infty)}{u_0^3}\ \ , \\ &\mathrm{Pr} = \frac{\nu}{\alpha},\ \ \mathrm{Sc} = \frac{\nu}{D},\ \ K = \frac{\nu\ K_l}{u_0^2} \end{aligned} \tag{6}$$

Eq. (1) to Eq. (4) are reduced to the following non-dimensional form

$$\frac{\partial U}{\partial X}+\frac{\partial V}{\partial Y}=0 \tag{7}$$

$$\frac{\partial U}{\partial t}+U\frac{\partial U}{\partial X}+V\frac{\partial U}{\partial Y}=\mathrm{Gr}\ T+\mathrm{Gc}\ C+\frac{\partial^2 U}{\partial Y^2} \tag{8}$$

$$\frac{\partial T}{\partial t}+U\frac{\partial T}{\partial X}+V\frac{\partial T}{\partial Y}=\frac{1}{\mathrm{Pr}}\ \frac{\partial^2 T}{\partial Y^2} \tag{9}$$

$$\frac{\partial C}{\partial t}+U\frac{\partial C}{\partial X}+V\frac{\partial C}{\partial Y}=\frac{1}{\mathrm{Sc}}\ \frac{\partial^2 C}{\partial Y^2}\ -\ K\ C\ . \tag{10}$$

The corresponding initial and boundary conditions in non-dimensional form are

$$\begin{aligned}
&t\le 0: \quad U=0,\ \ V=0,\ \ T=0,\ \ C=0\\
&t>0: \quad U=1,\ \ V=0,\\
&\qquad \frac{\partial T}{\partial Y}=-1,\ \ C=1 \quad \text{at } Y=0\\
&U=0,\quad T=0,\quad C=0, \quad \text{at } X=0\\
&U\to 0,\quad T\to 0,\quad C\to 0 \quad \text{as } Y\to\infty.
\end{aligned} \tag{11}$$

3 Finite-difference technique

The unsteady, non-linear coupled Eq. (7) to Eq. (10) with the condition (11) are solved by employing an implicit finite-difference scheme of Crank-Nicolson type. The finite-difference equations corresponding to Eq. (7) to Eq. (10) are as follows

$$\frac{\left[U^{n+1}_{i,j}-U^{n+1}_{i-1,j}+U^{n}_{i,j}-U^{n}_{i-1,j}+U^{n+1}_{i,j-1}-U^{n+1}_{i-1,j-1}+U^{n}_{i,j-1}-U^{n}_{i-1,j-1}\right]}{4\triangle X}+\frac{\left[V^{n+1}_{i,j}-V^{n+1}_{i,j-1}+V^{n}_{i,j}-V^{n}_{i,j-1}\right]}{2\triangle Y}=0 \tag{12}$$

$$\begin{aligned}
&\frac{\left[U^{n+1}_{i,j}-U^{n}_{i,j}\right]}{\triangle t}+U^{n}_{i,j}\frac{\left[U^{n+1}_{i,j}-U^{n+1}_{i-1,j}+U^{n}_{i,j}-U^{n}_{i-1,j}\right]}{2\triangle X}\\
&\quad+V^{n}_{i,j}\frac{\left[U^{n+1}_{i,j+1}-U^{n+1}_{i,j-1}+U^{n}_{i,j+1}-U^{n}_{i,j-1}\right]}{4\triangle Y}\\
&=\frac{\mathrm{Gr}}{2}\left[T^{n+1}_{i,j}+T^{n}_{i,j}\right]+\frac{\mathrm{Gc}}{2}\left[C^{n+1}_{i,j}+C^{n}_{i,j}\right]\\
&\quad+\frac{\left[U^{n+1}_{i,j-1}-2U^{n+1}_{i,j}+U^{n+1}_{i,j+1}+U^{n}_{i,j-1}-2U^{n}_{i,j}+U^{n}_{i,j+1}\right]}{2(\triangle Y)^2.}
\end{aligned} \tag{13}$$

$$\begin{aligned}
&\frac{\left[T^{n+1}_{i,j}-T^{n}_{i,j}\right]}{\triangle t}+U^{n}_{i,j}\frac{\left[T^{n+1}_{i,j}-T^{n+1}_{i-1,j}+T^{n}_{i,j}-T^{n}_{i-1,j}\right]}{2\triangle X}\\
&\quad+V^{n}_{i,j}\frac{\left[T^{n+1}_{i,j+1}-T^{n+1}_{i,j-1}+T^{n}_{i,j+1}-T^{n}_{i,j-1}\right]}{4\triangle Y}\\
&=\frac{1}{\mathrm{Pr}}\frac{\left[T^{n+1}_{i,j-1}-2T^{n+1}_{i,j}+T^{n+1}_{i,j+1}+T^{n}_{i,j-1}-2T^{n}_{i,j}+T^{n}_{i,j+1}\right]}{2(\triangle Y)^2}\ .
\end{aligned} \tag{14}$$

The thermal boundary condition at $Y=0$ in the finite-difference form is

$$\frac{1}{2}\ \frac{\left[T^{n+1}_{i,1}+T^{n}_{i,1}-T^{n+1}_{i,-1}-T^{n}_{i,-1}\right]}{2\ \triangle Y}=-1\ . \tag{15}$$

At $Y=0$ (i.e., j = 0) Eq. (14), becomes

$$\begin{aligned}
&\frac{\left[T^{n+1}_{i,0}-T^{n}_{i,0}\right]}{\triangle t}+U^{n}_{i,0}\ \frac{\left[T^{n+1}_{i,0}-T^{n+1}_{i-1,0}+T^{n}_{i,0}-T^{n}_{i-1,0}\right]}{2\triangle X}\\
&\quad=\frac{1}{\mathrm{Pr}}\frac{\left[T^{n+1}_{i,-1}-2T^{n+1}_{i,0}+T^{n+1}_{i,1}+T^{n}_{i,-1}-2T^{n}_{i,0}+T^{n}_{i,1}\right]}{2(\triangle Y)^2}\ .
\end{aligned} \tag{16}$$

After eliminating $T^{n+1}_{i,-1}+T^{n}_{i,-1}$ using Eq. (15), Eq. (16) reduces to the form

$$\begin{aligned}
&\frac{\left[T^{n+1}_{i,0}-T^{n}_{i,0}\right]}{\triangle t}+U^{n}_{i,0}\ \frac{\left[T^{n+1}_{i,0}-T^{n+1}_{i-1,0}+T^{n}_{i,0}-T^{n}_{i-1,0}\right]}{2\triangle X}\\
&\quad=\frac{1}{\mathrm{Pr}}\frac{\left[T^{n+1}_{i,1}-T^{n+1}_{i,0}+T^{n}_{i,1}-T^{n}_{i,0}+2\triangle Y\right]}{(\triangle Y)^2}
\end{aligned} \tag{17}$$

$$\begin{aligned}
&\frac{\left[C^{n+1}_{i,j}-C^{n}_{i,j}\right]}{\triangle t}+U^{n}_{i,j}\frac{\left[C^{n+1}_{i,j}-C^{n+1}_{i-1,j}+C^{n}_{i,j}-C^{n}_{i-1,j}\right]}{2\triangle X}\\
&\quad+V^{n}_{i,j}\frac{\left[C^{n+1}_{i,j+1}-C^{n+1}_{i,j-1}+C^{n}_{i,j+1}-C^{n}_{i,j-1}\right]}{4\triangle Y}\\
&\quad=\frac{1}{\mathrm{Sc}}\frac{\left[C^{n+1}_{i,j-1}-2C^{n+1}_{i,j}+C^{n+1}_{i,j+1}+C^{n}_{i,j-1}-2C^{n}_{i,j}+C^{n}_{i,j+1}\right]}{2(\triangle Y)^2}\\
&\quad-\frac{K}{2}(C^{n+1}_{i,j}+C^{n}_{i,j})\ .
\end{aligned} \tag{18}$$

The region of integration is considered as a rectangle with sides $X_{\max}(=1)$ and $Y(=14)$, where $Y_{\max}$ corresponds to $Y=\infty$, which lies very well outside the momentum, energy and concentration boundary layers. The maximum of Y was chosen as 14 after some preliminary investigations so that the last two of the boundary conditions (11) are satisfied. Here, the subscript i-designates the grid point along the X-direction, j-along the Y-direction and the superscript n along the t-direction. During any one time step, the coefficients $U^{n}_{i,j}$ and $V^{n}_{i,j}$ appearing in the difference equations are treated as constants. The values of C, T, U and V at time level $(n+1)$ using the known values at previous time level (n) are calculated as follows: The finite-difference equations (14) and (17) at every internal nodal point on a particular i-level constitute a tridiagonal system of equations. Such a system of equations are solved by using Thomas algorithm as discussed in Carnahan et al. [8]. Thus, the values of T are known at every internal nodal point on a particular i at $(n+1)$th time level. Similarly, the values of C and U are calculated from Eq. (18) and (13) respectively. Then the values of V are calculated explicitly using the Eq. (12) at every nodal point at particular i-level at $(n+1)$th time level. This process is repeated for various i-levels. Thus the values of C, T, U

and V are known, at all grid points in the rectangular region at $(n+1)$th time level.

Computations are carried out until the steady-state is reached. The steady-state solution is assumed to have been reached, when the absolute difference between the values of U as well as temperature T and concentration C at two consecutive time steps are less than 10^{-5} at all grid points. After experimenting with few set of mesh sizes, they have been fixed at the level $\triangle X = 0.05, \triangle Y = 0.25$, and the time step $\triangle t = 0.01$. In this case, spatial mesh sizes are reduced by 50% in one direction, and then in both directions, and the results are compared. It is observed that, when mesh size is reduced by 50% in X-direction and Y-direction the results differ in fourth decimal places. Hence, the above mentioned sizes have been considered as appropriate mesh sizes for calculation.

The local truncation error is $O(\triangle t^2 + \triangle Y^2 + \triangle X)$ and it tends to zero as $\triangle t, \triangle X$ and $\triangle Y$ tend to zero. Hence the scheme is compatible. The finite-difference scheme is unconditionally stable as discussed in Muthucumaraswamy and Ganesan [5]. Stability and compatibility ensures convergence.

4
Results and discussion

Representative numerical results for the uniform surface heat flux and mass diffusion will be discussed in this section. In order to ascertain the accuracy of the numerical results, the present study is compared with the available exact solution in the literature. The concentration profiles for $K = 0.2$, $\mathrm{Sc} = 0.7, 0.9, \mathrm{Gr} = 2, \mathrm{Gc} = 5$ and $\mathrm{Pr} = 0.71$ (corresponding to $\eta = Y/2\sqrt{t}$) are compared with the available exact solution of Das et al. [7] at $t = 0.2$ in Fig. 1 and they are found to be in good agreement. The finite-difference equation (18) can be adjusted to meet these circumstances if one takes

(i) $K > 0$ for the destructive reaction,
(ii) $K < 0$ for the genearative reaction,
(iii) $K = 0$ for no reaction.

The transient velocity profiles for different chemical reaction parameter and Schmidt number are shown in fig. 2. The velocity profiles presented are those at $X = 1.0$. It is observed that for $\mathrm{Pr} = 0.71, \mathrm{Gr} = 2$, $\mathrm{Gc} = 5, \mathrm{Sc} = 0.6$ and $K = -2.0$, the velocity increases with time, reaches a temporal maximum around time $t = 0.8$ and becomes steady at time $t = 6.3$. It is observed that the velocity increases during generative reaction and decreases in destructive reaction. It is clear that the velocity increases with decreasing values of Schmidt number or chemical reaction parameter. The time taken to reach the steady-state increases with increasing the Schmidt number or the chemical reaction parameter. However, the time required for the velocity to reach steady-state depends upon both Schmidt number and chemical reaction parameter. The contribution of mass diffusion to the buoyancy force increases the maximum velocity significantly. The steady-state velocity profiles for different thermal Grashof number, mass Grashof number and Prandtl number are shown in Fig. 3. It is observed that the velocity increases with increasing thermal Grashof number or mass Grashof number and decreases with increasing Prandtl number.

The transient and steady-state temperature for different values of Prandtl number and chemical reaction parameter are shown in Fig. 4. The effect of Prandtl number is very important in temperature profiles. It is observed that the temperature increases with increasing values of chemical reaction parameter, and decreasing values of Prandtl number.

The effect of chemical reaction parameter and Schmidt number are very important in concentration field. The transient and steady-state concentration profile for different chemical reaction parameter are shown in Fig. 5. There is a fall in concentration due to increasing values of the chemical reaction parameter. The concentration profiles for different values of thermal Grashof number, mass Grashof number and Schmidt number are shown in Fig. 6. It is observed that the concentration increases with

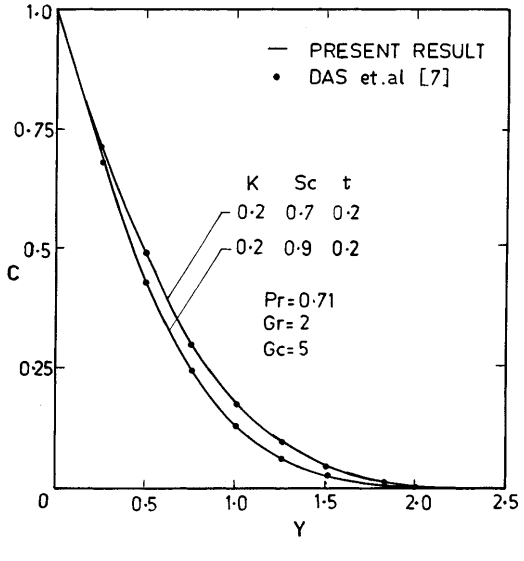

Fig. 1. Comparison of concentration profiles

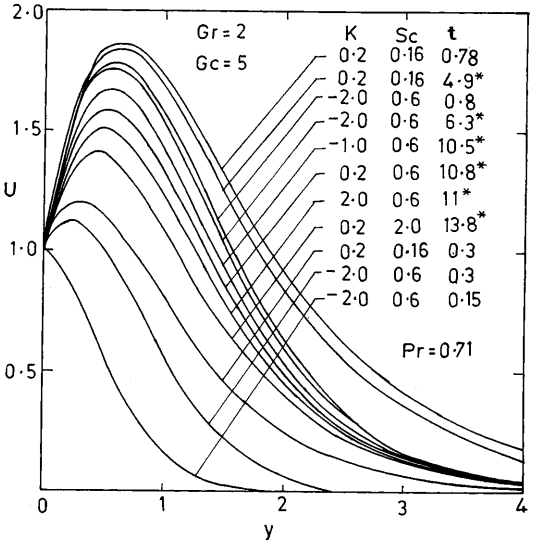

Fig. 2. Transient velocity profiles at $X = 1.0$ for different Sc and K (*steady-state value)

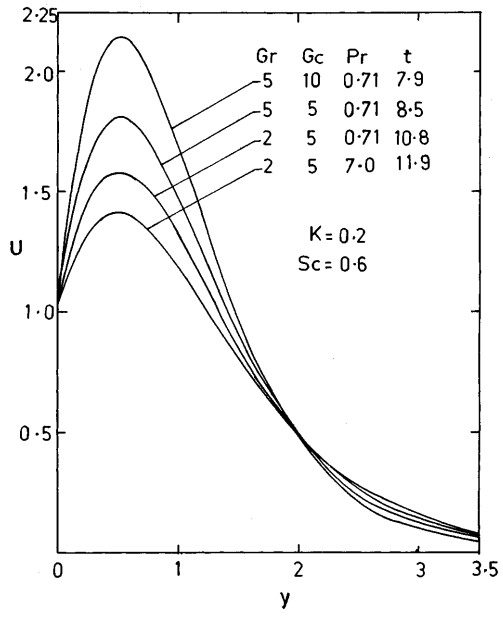

Fig. 3. Steady-state velocity profiles at $X = 1.0$ for different Gr, Gc and Pr

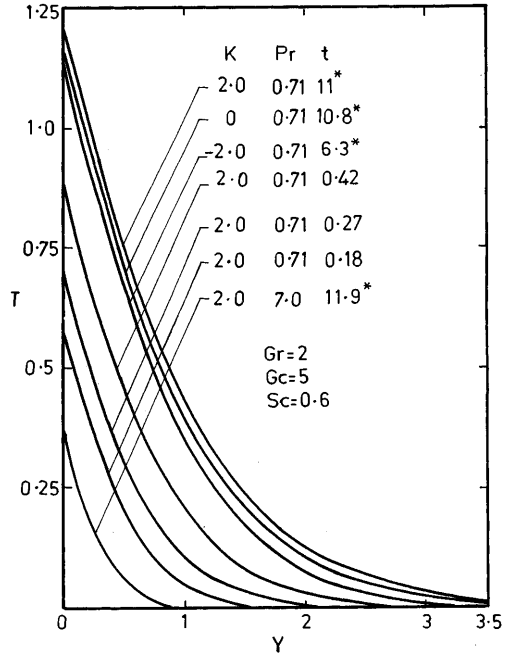

Fig. 4. Transient temperature profiles at $X = 1.0$ for different K and Pr (*steady-state value)

decreasing Schmidt number or thermal Grashof number or mass Grashof number.

$$\tau_X = -\left(\frac{\partial U}{\partial Y}\right)_{Y=0} \tag{19}$$

$$\bar{\tau} = -\int_0^1 \left(\frac{\partial U}{\partial Y}\right)_{Y=0} \mathrm{d}X \tag{20}$$

$$\mathrm{Nu}_X = -X\left[\frac{\left(\frac{\partial T}{\partial Y}\right)_{Y=0}}{T_{Y=0}}\right] \tag{21}$$

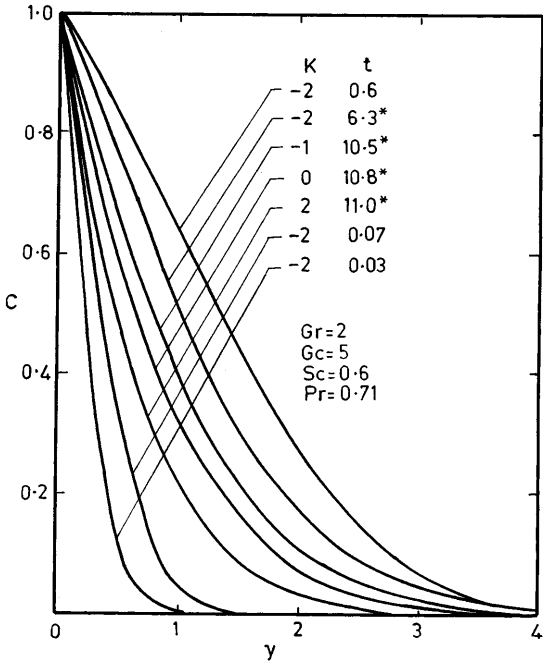

Fig. 5. Transient concentration profiles at $X = 1.0$ for different K (*steady-state value)

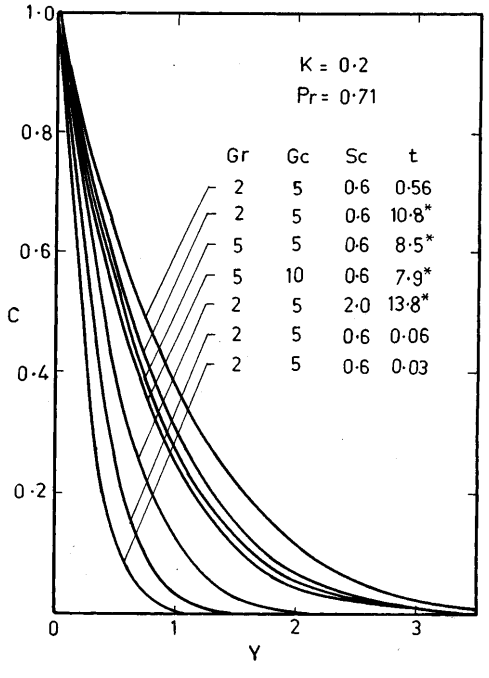

Fig. 6. Transient concentration profiles at $X = 1.0$ for different Gr, Gc and Sc (*steady-state value)

$$\overline{\mathrm{Nu}} = -\int_0^1 \left[\frac{\left(\frac{\partial T}{\partial Y}\right)_{Y=0}}{T_{Y=0}}\right] \mathrm{d}X \tag{22}$$

$$\mathrm{Sh}_X = -X\left(\frac{\partial C}{\partial Y}\right)_{Y=0} \tag{23}$$

$$\overline{\mathrm{Sh}} = -\int_0^1 \left(\frac{\partial C}{\partial Y}\right)_{Y=0} \mathrm{d}X \ . \tag{24}$$

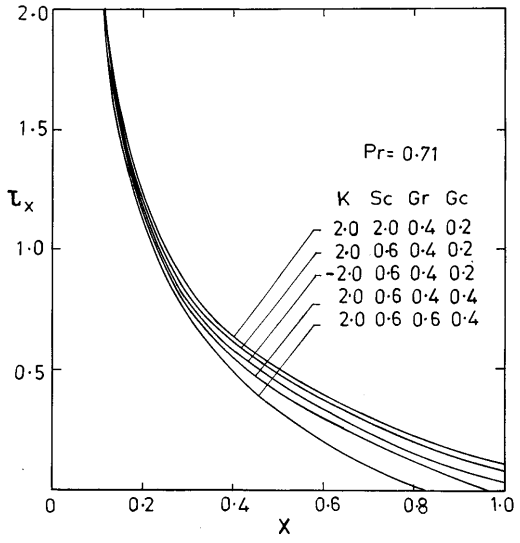

Fig. 7. Local skin-friction

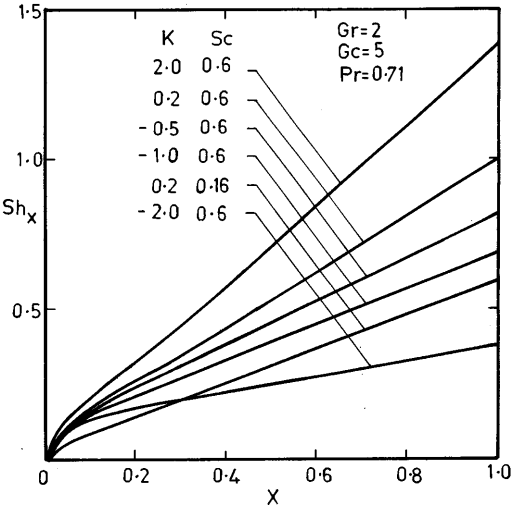

Fig. 9. Local Sherwood number

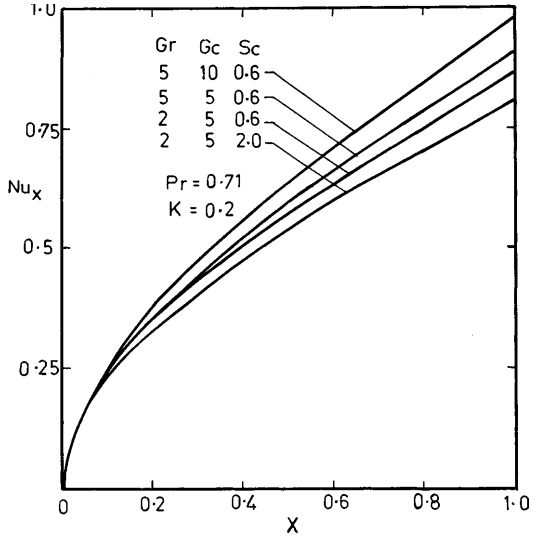

Fig. 8. Local Nusselt number

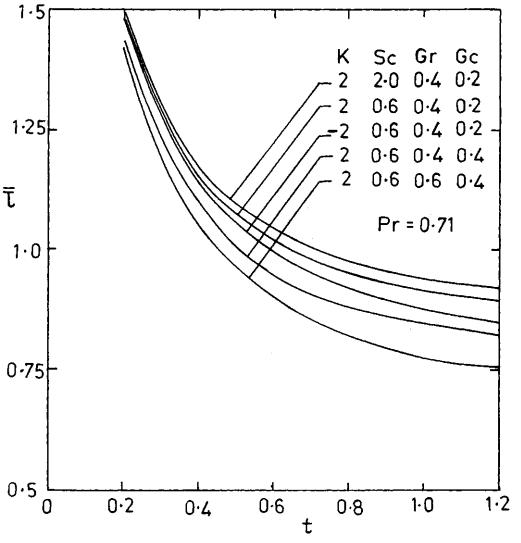

Fig. 10. Average skin-friction

The derivatives involved in the Eq. (19) to Eq. (24) are evaluated using five-point approximation formula and then the integrals are evaluated using Newton-Cotes closed integration formula.

The local skin-friction values are evaluated from Eq. (19) and plotted in Fig. 7 as a function of the axial coordinate X. Local skin-friction decreases as X increases. The local wall shear stress increases with decreasing values of the thermal Grashof number or the mass Grashof number. It is observed that the skin-friction increases with increasing the value of the chemical reaction parameter or Schmidt number. The local Nusselt number for different thermal Grashof number, mass Grashof number and Schmidt number are shown in Fig. 8. The rate of heat transfer increases with increasing thermal Grashof number or mass Grashof number and decreases with increasing Schmidt number. This trend is just opposite in local Sherwood number with respect to the Schmidt number, because, the concentration profiles decrease with increasing values of Sc, near the plate. The Local Sherwood number for different values of Schmidt number and chemical reaction parameter are shown in Fig. 9. It is observed that local Sherwood increases with increasing Schmidt number. The rate of concentration increases during destructive reaction and decreases in generative reaction.

The effects of Gr, Gc, Sc and the chemical reaction parameter on the average values of the skin-friction, the Nusselt number and the Sherwood number are shown in Figures 10, 11 and 12 respectively. The average skin-friction increases with decreasing Gr or Gc and increases with increasing the Schmidt number throughout the transient period. The average Nusselt number increases with decreasing Sc and it increases with increasing Gr or Gc. The average Sherwood number increases with increasing the chemical reaction parameter.

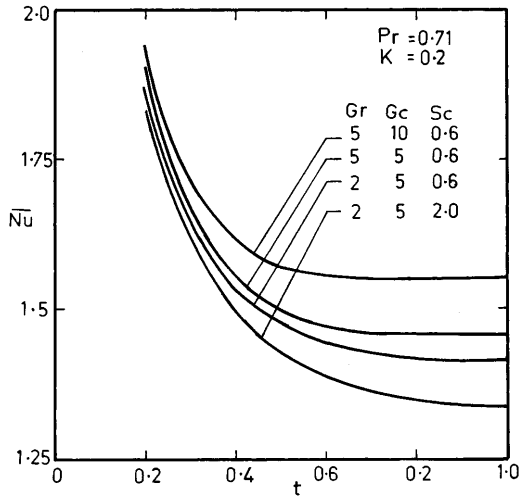

Fig. 11. Average Nusselt number

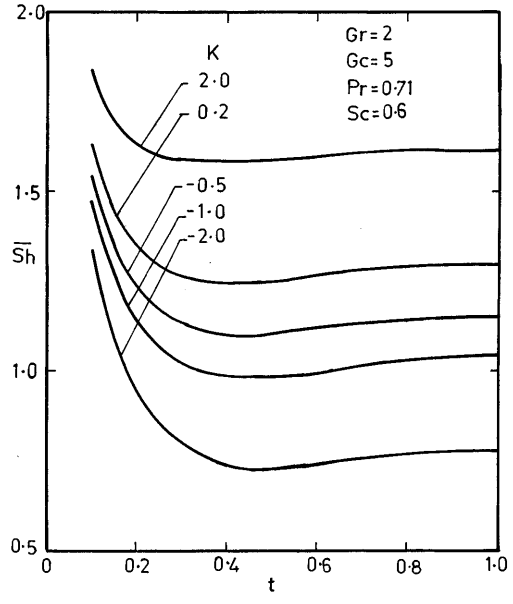

Fig. 12. Average Sherwood number

5
Conclusions

A detailed numerical study has been carried out for the flow past an impulsively started semi-infinite vertical plate with uniform heat flux and diffusion of chemically reactive species. The dimensionless governing equations are solved by an implicit finite-difference scheme of Crank-Nicolson type. The fluids considered in this study are air and water. This study has been compared with available exact solution in the literature and they are found to be in good agreement. It is observed that the velocity and concentration increases during generative reaction and decreases in destructive reaction. It is found that the number of time steps to reach steady-state depends strongly on the chemical reaction parameter.

References

1. **Stokes GG** (1851) On the effect of internal friction of fluids on the motion of pendulums. Camb. Phil. Trans., IX 8–106
2. **Hall MG** (1969) Boundary layer over an impulsively started flat plate. Proc. of the Royal Society London, 310A: 410–414
3. **Soundalgekar VM** (1977) Free convection effects on the Stokes problem for an infinite vertical plate. ASME Journal of Heat Tranfer, 99, 499–501
4. **Soundalgekar VM** (1979) Effects of mass transfer and free convection currents on the flow past an impulsively started vertical plate. ASME Journal of Applied Mechanics, 46, 757–760
5. **Muthukumaraswamy R, Ganesan P** (1998) Unsteady flow past an impulsively started vertical plate with heat and Mass Tranfer. Heat and Mass Transfer, 34, 187–193
6. **Soundalgekar VM, Birajdar NS, Darwekar VK** (1984) Mass Transfer effects on the flow past an impulsively started infinite vertical plate with variable temperature or constant heat flux. Astrophysics and Space Science, 100, 159–164
7. **Das UN, Deka R, Soundalgekar VM** (1994) Effects of Mass transfer on flow past an impulsively started infinite vertical plate with constant heat flux and chemical reaction. Forschung im Ingenieurwesen- Engineering Research, 60, 284–287
8. **Carnahan B, Luther HA, Wilkes JO** (1969) Applied Numerical Methods, John Wiley & Sons, New York
9. **Byron Bird R, Warren E. Stewart, Edwin N. Lightfoot** (1960) Transport Phenomena, John Wiley & Sons, New York